International Journal of Microwave and Wireless Technologies

cambridge.org/mrf

Reconfigurable planar leaky wave antenna composed of rectangular conducting patches

Jan Machac, Milan Svanda and Vaclav Kabourek

Faculty of Electrical Engineering, Czech Technical University in Prague Technicka, Prague 6, Czech Republic

Research Paper

Cite this article: Machac J, Svanda M, Kabourek V (2025) Reconfigurable planar leaky wave antenna composed of rectangular conducting patches. *International Journal of Microwave and Wireless Technologies* **17**(3), 428–436. https://doi.org/10.1017/S1759078725000327

Received: 23 July 2024
Revised: 24 February 2025
Accepted: 27 February 2025

Keywords:
antenna array; leaky wave antenna; reconfigurable antenna; varactor

Corresponding author: Jan Machac; Email: machac@fel.cvut.cz

Abstract

A reconfigurable leaky-wave antenna and its application capable of electronically steering the beam within the entire hemisphere is presented. The original antenna is designed as a 1D array of conducting patches on a dielectric substrate coupled by varactors in series with interdigital capacitors. The beam of this antenna is driven by a DC bias that controls the capacitances of the varactor diodes over a frequency range from 8 to 8.2 GHz. Simulations showed a change in the direction of the main radiation pattern within 55° at 8 GHz by varying the varactor capacitances in the range of 0.1 to 1 pF. The maximum gain is 10 dBi and the side lobe level is -10 dB. The fabricated antenna sample operates at an applied DC voltage between 0 and 12 V, which corresponds to varactor capacitances controlled in the range of 1 to 0.15 pF. This gives a range of elevation angles equal to 40°. The application of the antenna in a reconfigurable star-type structure is proposed. The direction of the main lobe of the radiation pattern in azimuth is controlled by switching between the centrally excited eight antenna arrays using PIN diodes. The direction of radiation in elevation is controlled by the DC bias of the varactors of a particular array switched to "ON". This complex beam steering throughout the hemisphere represents a novel character of the presented antenna. The antenna has a planar structure. Low-cost printed circuit board technology was used for its fabrication.

Introduction

Antenna arrays designed as traveling wave antennas have the advantage of a relatively wide operating bandwidth compared to resonant antennas. Leaky wave antennas (LWAs) are a broad class of travelling wave antennas that are often designed as composite right/left-handed (CRLH) transmission lines [1] and that are capable of radiating both forward and backward waves depending on the frequency of the feed signal. These arrays can be constructed as arrays of rectangular conducting arrays known as mushroom cells [2].

For many applications it is advantageous to control the direction of the main antenna beam by some external means, usually electronically using a DC voltage, so reconfigurable antennas are used in these applications.

Over the last 20 years, a number of approaches have been studied to achieve reconfigurability. In the survey [3], the most important works and advances in the field of reconfigurable elements were presented, with the main focus on antennas with clear practical applications in the emerging areas of millimeter wave, 5G/6G communications, IoT, etc.

Typical elements controlling the radiation pattern of the antenna are varactors, in which the p-n junction capacitance is controlled by a DC bias varying the thickness of the depletion layer of the junction. The first information on reconfigurable LWAs with radiation pattern controlled by DC bias varactors was reported in [4]. The presented antenna exhibited a beam sensed by a DC voltage in the range of 0 to 20 V from −49° to 50° at 3.33 GHz. In [5], an LWA based on a corrugated substrate integrated waveguide (C-SIW) with beam steering capability was presented. The beam is steered within 72° from backward to forward direction at 4.5 GHz using varactors operated by a DC bias in the interval 7.5–32 V. The LWA presented in [6] was composed of a corrugated microstrip line loaded with varactor diodes. The beam was steered within 45° from the backward to the forward direction at 4.5 GHz using varactors operated by a DC bias boosted up to 20 V. A beam scanning circularly polarized LWA was presented in [7]. The structure consisted of a CRLH transmission line. Varactor diodes steered the beam continuously from −17° to +40°. The antenna operated at 2.4 GHz. A reconfigurable array of unit cells with varactor load was presented in [8]. The varactors were fed individually using an optimized biasing scheme. A very wide sensing range equivalent to 130° was achieved.

© The Author(s), 2025. Published by Cambridge University Press in association with The European Microwave Association.

Another way of electronically controlling the antenna beam can be achieved by using liquid crystals, as done by the authors [9]. In the proposed antenna, the SIW transmission line was used. The gap between the middle SIW conductor and the top conductor was filled with liquid crystals. The beam was steered within 30° at a frequency of 52 GHz. The substrate of the antenna presented in [10] was formed by liquid crystals, which directly changed its permittivity. The beam was driven within 24° at a frequency of 30 GHz. The reflect array antenna composed of an array of 55 × 55 elements based on liquid crystal technology was proposed in [11]. This antenna exhibited a scanning range of 35° at a frequency of 98 GHz.

The coplanar waveguide (CPW) LWA was introduced in [12]. The beam was steered by MEMS crossing slots in the CPW center strip. This antenna presented an extreme scanning capability 126°, from −73° (backward wave) to 53 (forward wave) at 77 GHz.

The reconfigurable SIW LWA, which was presented in [13], exhibited a wide scanning range of the 99° beam at 5.98 GHz. The slot period of this antenna was varied electronically by switching between ON and OFF states of the PIN diodes. This changed the phase constant of the higher order spatial harmonics and controlled the beam direction.

The technology of monolithic integration of 11 × 11 metal arrays controlled via 208 thin-film transistor switches was used to design the reconfigurable antenna in [14]. The beam was steered in elevation through 90° at a frequency of 2.1–2.5 GHz.

An electronically reconfigurable antenna with beam steering using an embedded RF PIN was proposed in [15], operating at 5.8 GHz. This antenna did not offer continuous scanning, but three operating modes in which the antenna operates with the beam directed to – 30°, 0° and 30° elevation.

A Wi-Fi smart antenna was introduced in [16]. The design is based on the electromagnetic complementary Huygens principle. The omnidirectional and end fire directional radiation patterns were obtained by controlling the states of the mushroom cells using two PIN diodes, therefore the antenna switched between two important operating modes of the Wi-Fi system.

Beam steering in the azimuthal plane is often solved by switching the beam into individual sectors using several emitters. PIN diodes are usually used for this purpose. In [17], four sectors were used using four leaky-wave antennas. In [18], eight switchable Vivaldi type radiators were used providing radiation to eight switchable azimuthal sectors. The antenna proposed in [19] demonstrated 360° azimuthal scanning performed in four sectors, requiring only four array elements for beam switching. Four low-profile, wide-bandwidth edge antipodal antennas were used to realize the four-element radiation pattern. The authors of [20] presented a reconfigurable planar antenna with beam switching and filtering capability. The structure was designed using SIW technology. By integrating PIN diodes, the structure effectively divided the azimuthal plane into eight sectors, which enabled a reconfigurable pattern within 360°. The operating frequency of the proposed antenna was 12.7–13.3 GHz. The Alford loop antenna was used in [21, 22]. Here, the sensing resolution is finer depending on the number of activated line segments located on the antenna perimeter. In all these antennas with azimuthal beam steering, the beam was steered in elevation by changing the frequency.

The ultimate goal of the research described in this paper is to design and implement a 1D antenna array that is fed at a

Table 1. Presented results compared with reconfigurable LW arrays taken from literature

Reference	[4]	[5]	[6]	[7]	[8]	[13]	[11]	[30]	This work
Variation of maximal radiation direction (deg)	99	72	45	57	130	99	35	35	55
Maximal gain (dBi)	18	5.6	13.7	4.9	8.9	5.5	25	12	10
Side lobe level (dB)	−10	−10	−10	−10	−10	−10	−9	−20	−10
Frequency band (GHz)	3.3	4.5	5.5–5.8	2.4	10	5.98	98	5.3–6	8–8.2*
DC bias range (V)	0–20	7.5–32	0–20	3.5–6.5	Opt.	Coding PIN	55 × 55 biased cells	2–12	0–12
Electric length (λ_o)	2.2	3.6	6.24	3.35	4	6.7	22 × 22	6.42	3.36

*The antenna radiation pattern is steered as described in Figs. 4 and 9 in this frequency band.

https://doi.org/10.1017/S1759078725000327 Published online by Cambridge University Press

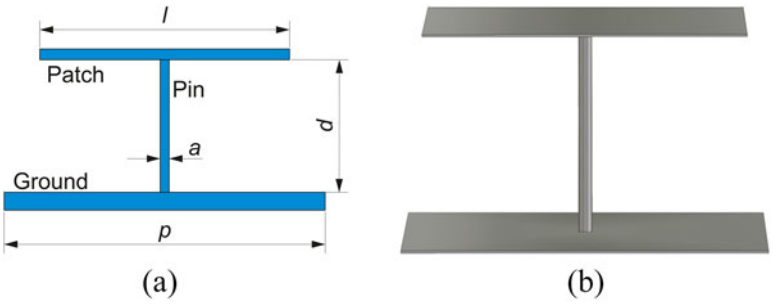


Figure 1. Unit cell of the antenna. (a) Dimensions, (b) view of the cell with the invisible dielectric substrate.

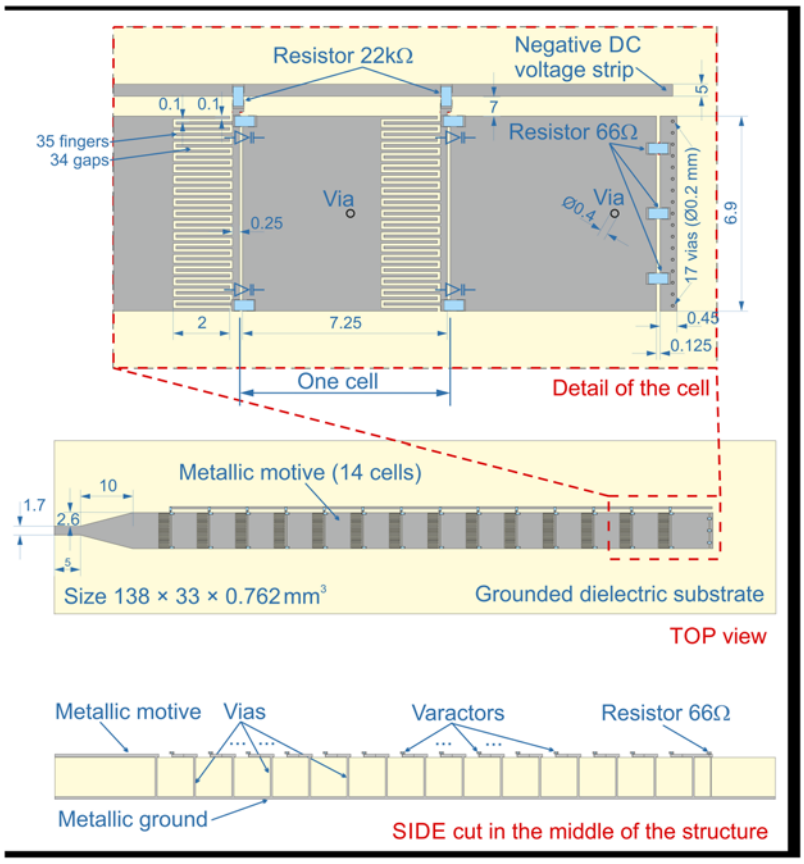


Figure 2. Sketch of antenna with a detail of the cell with included varactors and resistors.

single point but has continuously steerable radiation patterns in elevation at a constant frequency. The antenna consists of mushroom-shaped cells. This work is based on a modification of the reconfigurable LWA presented by the authors in [23]. The array has been redesigned to allow the connection of varactors, which allows the use of only one DC voltage source. This is due to the etched interdigital slots that cut through the conducting patches located on the dielectric substrate. The simulation results were verified by experiments, which demonstrated the effectiveness of the design. By varying the capacitances of the used varactors between 0.1 and 1 pF, the proposed LWA exhibits a change in the main lobe direction of the radiation pattern from 20° to 75° in the direct direction, i.e., within 55° in the frequency interval from 8 to 8.2 GHz. Measurements of the constructed antenna sample showed a narrower range of elevation angles at the selected DC voltages between 12 and 0 V equal to 40°. The measured maximum gain is 9 dBi, while the simulation shows 10 dBi. A comparison of the obtained results with some data reported in the literature is shown in Table 1.

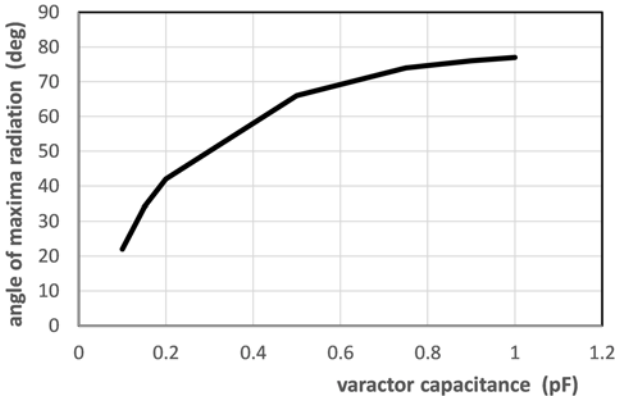


Figure 3. Calculated dependence of the angle of maximal radiation on the varactor capacitance at 8 Ghz.

https://doi.org/10.1017/S1759078725000327 Published online by Cambridge University Press

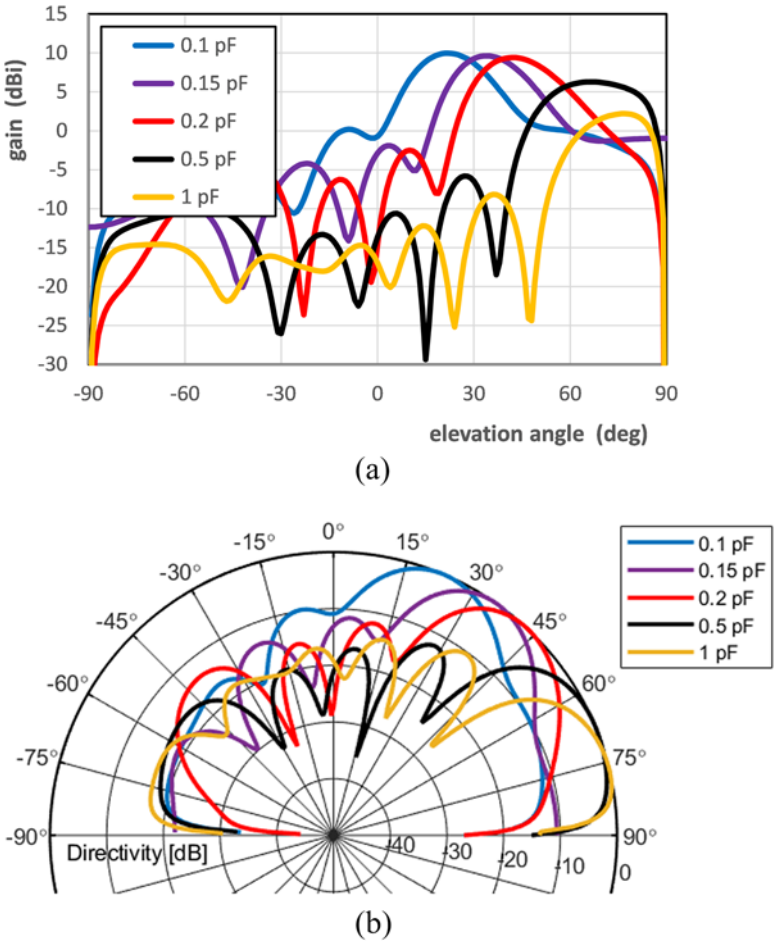


Figure 4. Calculated radiation patterns of the array at selected varactor capacitances at 8 Ghz. (a) Gain in rectangular coordinates, (b) normalized directivity in polar coordinates.

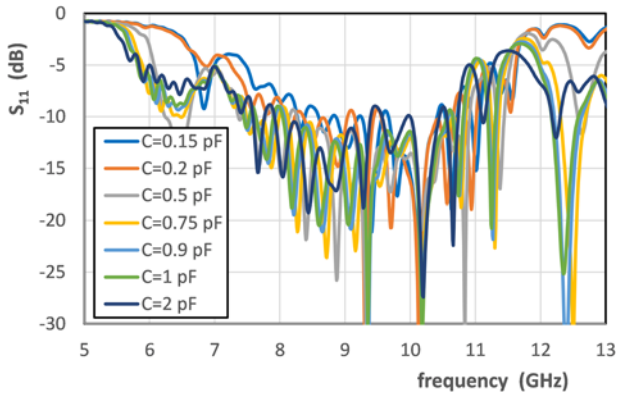


Figure 5. Calculated S_{11} of the antenna array for selected varactor capacitances.

The presented antenna array has a wide range of applications in systems requiring reconfigurable functions. The paper proposes this antenna array as part of a star structure antenna. Eight specific antenna arrays are connected in a star and are centrally excited. Eight PIN diodes select the radiation pattern of one of the antenna arrays. Thus, the structure radiates in the azimuthal plane in eight specific sectors covering 360°. The direction of radiation is controlled in elevation by the DC varactor bias of the antenna array, which is switched on. The whole structure was simulated in the CST Microwave Studio software. The results obtained show the control of the direction of the main radiation lobe throughout the half-space.

Design of a varactor-controlled LWA

A rectangular conducting patch known as a mushroom cell [2] is shown in Fig. 1. It is used as the basic cell of the proposed LWA array. This array works as a CRLH. The parallel inductances of the L_L are represented by the central pins. The series capacitances C_L are represented by the slots between the edges of the rectangular array cells. Such a line is capable of transmitting a leaky wave, which behaves as a backward wave below the resonant frequency (the phase constant is negative here) and behaves as a forward wave above the resonant frequency (the phase constant is positive here). For a balanced line where the series and parallel resonant frequencies are equal, the phase constant is equal to

$$\beta = \frac{1}{j\omega}\left(\omega\sqrt{C_R L_R} - \frac{1}{\omega\sqrt{C_L L_L}}\right), \quad (1)$$

where C_R (parallel capacitance) and L_R (serial inductance) are the parameters of the host transmission line. The antenna has been designed to radiate in the forward direction, i.e. above the resonant frequency, because of its intended use as an antenna radiating to the full hemisphere described in "The antenna with the beam steered in the whole hemisphere" section.

https://doi.org/10.1017/S1759078725000327 Published online by Cambridge University Press

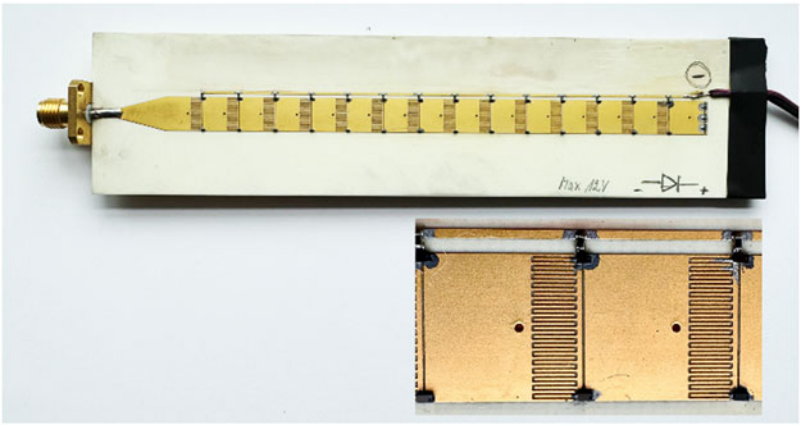


Figure 6. The fabricated antenna photo with the detailed view of the cell.

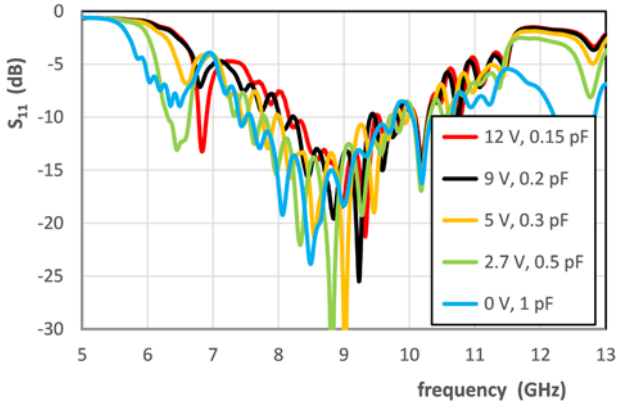


Figure 7. Measured S_{11} of the antenna array for selected varactor voltages.

The design of the basic LW antenna array with mushroom-shaped cells was presented in [23]. We have chosen a low-loss dielectric substrate with a thickness of $d = 0.762$ mm with a relatively low permittivity of 3.48 and tan $\delta = 0.0037$, the thickness of the plating is equal to 0.035 mm. In order to obtain the effective radiation in the forward direction in the frequency band around the desired value of 8 GHz, we obtained the following cell parameters based on simulations in CST Microwave Studio (CST MWS) [24]: the pin diameter $a = 0.4$ mm, the ground plane area is 7×7 mm, and the patch size is equal to 6.9×6.9 mm, so that the gaps between the patch edges are 0.1 mm wide.

The cell has been modified to incorporate varactors that control the emitted beam by changing its capacity. Two varactors are attached to each slot between the arrays. For simple operation of the antenna, only one voltage source needs to be used, so the varactors must be connected in parallel to a DC voltage. Therefore, the conductive top patches are slotted with interdigital capacitors (IDCs) that isolate the negative ports of the varactors from the ground to which the positive ports are connected. These IDCs reduce the capacitances between the arrays and de-tune the arrays originally designed without varactors. The IDC layout was adjusted using CST MWS simulations to bring the radiation frequency back to 8 GHz. This results in IDC finger lengths equal to 2 mm and slit widths equal to 0.1 mm. There are 35 fingers in each IDC. The arrangement of the cells and array terminations is shown in detail in Fig. 2 with the basic dimensions marked.

A new form of antenna termination was used. It consists of a parallel combination of three 66 Ω resistors connected through a set of 17 conductive shunts of 0.2 mm diameter to ground. These resistors model the Bloch impedance of the array determined by [25], which is approximately 20 Ω. This termination eliminates the need for a second port that would be matched without reflection. The antenna array is composed of 14 elements to achieve sufficient traveling wave drop across its entire length. The width of the 50 Ω microstrip feed line is 1.7 mm.

Adjacent cells are connected by two varactors that bridge the gap between them. In series with these two varactors, a resistor 22 kΩ is connected to the negative DC voltage strip (see detail in Fig. 2). In this way, all varactors are connected in parallel and only one DC voltage source can be used. The varactors used in the system are MA46H120 varactors from Macom [26]. These varactors operate with DC voltages in the range of 0 to 12 V with a corresponding capacitance change from 1 to 0.15 pF. The varactor diodes are represented in the CST MWS model by a single p-n junction capacitor only. The dependence of capacitances on DC bias voltage is given in [26].

The increased capacities of the embedded varactors shift the radiation maximum of the antenna array forward. The array shall be part of a finite star structure placed on a single substrate; see Fig. 10. The individual arrays will be fed at the center of the star and must therefore radiate towards the perimeter of the structure. The dependence of the maximum radiation angle on the varactor capacitance, calculated using the CST MWS, is plotted in Fig. 3 for a frequency of 8 GHz.

The radiation patterns calculated by CST MWS at 8 GHz are plotted in Fig. 4 for selected values of varactor capacitances. The angle $\theta = 0^\circ$ corresponds to the broad radiation. Positive angles represent the forward direction. Figure 4 shows the approximate 55° range of elevation angles for capacitance values from 0.1 to 1 pF. It coincides with Fig. 3. The radiation is directed forward. Unfortunately, increasing the varactor capacitances reduces the gain of the antenna.

The calculated input reflectivity S_{11} versus frequency for the selected varactor capacitances is shown in Fig. 5. The antenna can operate with a sufficient reflection coefficient value in the frequency band from 8 to 10.5 GHz. The exact bandwidth depends on the varactor capacity value. Increasing capacity widens this frequency band.

The varactor-controlled antenna array behaves similarly to a standard LWA array at the selected varactor DC bias values. The

https://doi.org/10.1017/S1759078725000327 Published online by Cambridge University Press

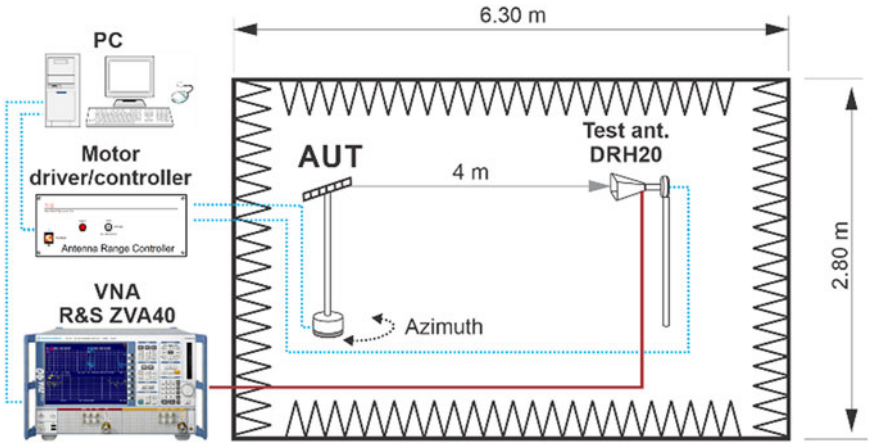


Figure 8. Antenna radiation pattern measurement setup in the full anechoic chamber.

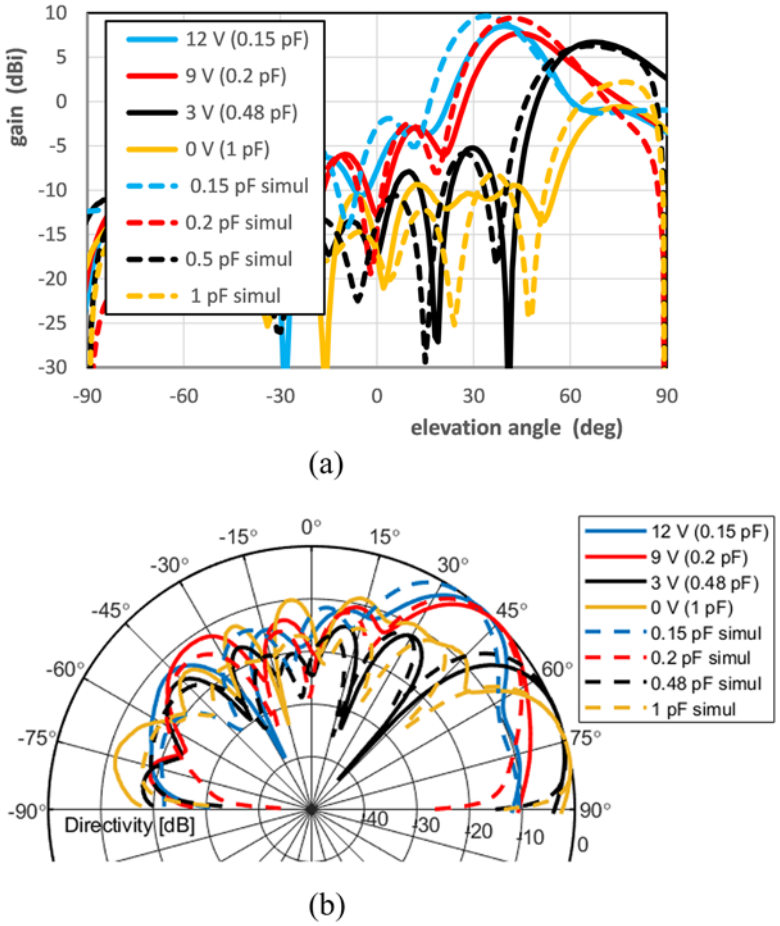


Figure 9. Measured radiation patterns of the antenna array at 8 Ghz for selected varactor voltages. Dashed lines represent simulated data for corresponding capacitance values. (a) Gain in rectangular coordinates, (b) normalized directivity in polar coordinates.

direction of maximum radiation is controlled by increasing the frequency in the forward direction.

Experiment

The antenna array designed in "Design of a varactor-controlled LWA" section was fabricated using a standard PCB process. Rogers RO4350B substrate material [27] with the parameters defined above was used. The structure is shown in Fig. 6. The varactors are connected across the slots at the conducting patch edges. The resistors 22 kΩ are connected between the patch edges and the negative DC voltage strip. The better view of this circuit is in the detail of Fig. 2. In this way, all varactors are connected in parallel and only one DC voltage source can be used.

S_{11} measured over a wide frequency band of 5–13 GHz is plotted in Fig. 7. The measurements were performed using a Rohde & Schwarz ZVA40 vector network analyzer (VNA) for selected voltages in the range 0–12 V. The voltages used correspond to varactor capacitances taken from [26]; see the legend of the graph. It can be seen that the measured data of S_{11} agrees well with the calculated data plotted in Fig. 5.

https://doi.org/10.1017/S1759078725000327 Published online by Cambridge University Press

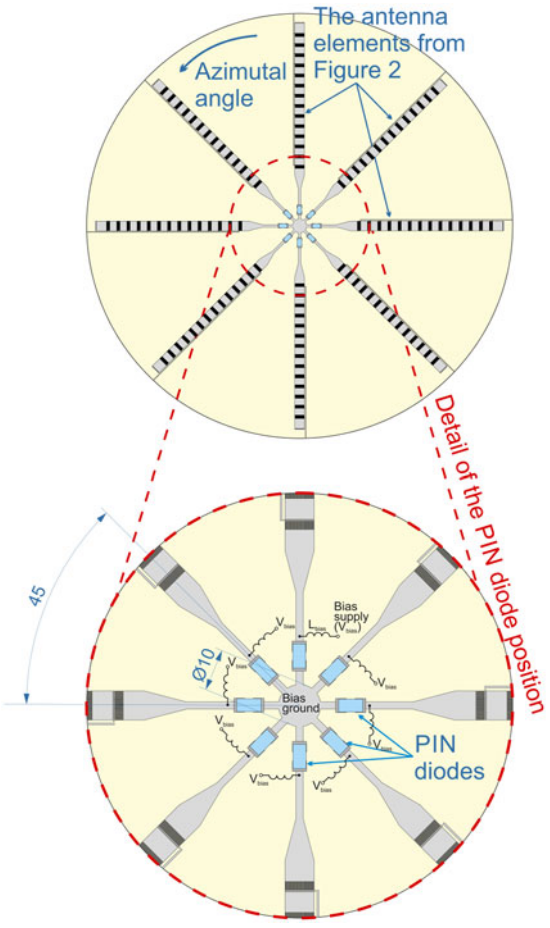


Figure 10. The star antenna layout with the beam steered in the whole hemisphere.

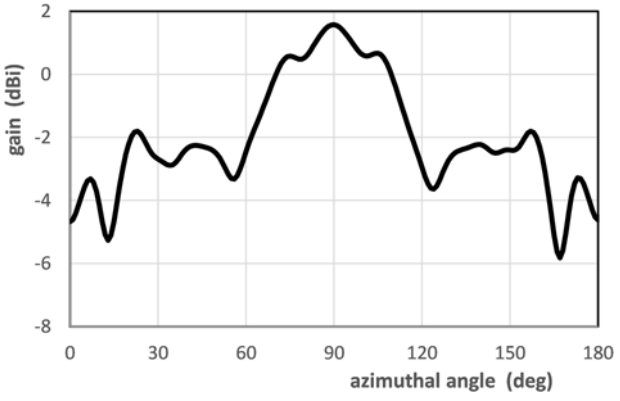


Figure 11. The radiation pattern in the azimuthal plane of the antenna presented in Figure 10. Frequency is 8 Ghz, varactor capacitances are 1 pf. Only one antenna is switched "ON," all other are in the "OFF" state.

The antenna radiation patterns were measured in a full anechoic chamber using the NSI automatic scanning system for the far-field controlled by the NSI 2000 measurement software [28]. A Rohde & Schwarz ZVA40 dual-port VNA was used to measure the transmission coefficient S_{21} between the antenna under test and the DRH20E test horn antenna [29]. The gain was determined by the gain transfer method using a calibrated DRH20E antenna with a known gain. The radiation pattern measurement setup is shown in Fig. 8.

The radiation patterns measured at 8 GHz are plotted in Fig. 9 for selected DC bias voltages of varactors between 12 and 0 V. This gives the range of elevation angles 40°. Extrapolating the radiation pattern measured at 12 V, which corresponds to a varactor capacitance of 0.15 pF, to a voltage corresponding to a capacitance equal to 0.1 pF yields the range of elevation angles 50°, which corresponds to the simulated value 55°. The measured maximum gain is approximately 9 dBi. The measured side lobe level (SLL) is approximately −10 dB. Fig. 9 compares the measured and simulated data at DC voltages equal to 12 V and 0 V corresponding to 0.15 pF and 1 pF. The curves are similar except for the gain maximum.

The measured radiation patterns shown in Fig. 9 do not change as the frequency increases up to 8.2 GHz. Increasing the frequency further causes a narrowing of the range of elevation angles along with a decrease in the maximum gain at low values of the applied DC voltage.

Table 1 summarizes the details of selected reconfigurable antennas that have been reported in the literature. Our design offers an antenna with a wider controllable range of maximum radiation angle than previous designs [23, 30]. The gain of 10 dBi is higher than most of the presented designs, and the SLL equal to −10 dB is similar to the antennas presented in Table 1. The used range of DC control voltage values of 0–12 V is due to the varactors MA46H120 [26] needed to provide relatively low capacitances to control effectively the radiation in elevation. The presented structure has relatively compact dimensions 3.36 × 0.88 λ_0. The antenna presented in [11] needs very complex drivers controlling the individual liquid crystal cells. Its electrically large structure corresponds to a large gain.

The antenna with the beam steered in the whole hemisphere

The reconfigurable antenna array presented, see Figs. 2 and 6, was designed as part of an antenna with electronically controlled radiation at a constant frequency throughout the hemisphere. The arrangement of this antenna is shown in Fig. 10. The eight antennas are connected in a star geometry and are fed centrally. They are switched "ON" by PIN diodes. This switching determines the direction of radiation to selected sectors in the azimuthal plane. The radiation pattern calculated by the CST MWS at 8 GHz is plotted in Fig. 11. The horizontal left-facing array is switched "ON" and all other antennas are disconnected by PIN diodes in the "OFF" state. The capacitances of all varactors are set to 1 pF. At this value of the varactor capacitances, the antenna radiates almost in the plane of the substrate surface at an elevation angle equal to 80°, see Figs. 4 and 9. The direction of radiation in elevation is controlled, as described above, by the DC bias determining the capacitances of the varactors used, see the simulation results shown in Fig. 4 and the measured results shown in Fig. 9. The radiation patterns when the other specific antennas are "ON" are similar due to the structure symmetry.

Figure 10 schematically indicates the possible location of the bias for PIN diode switching. The central circular conducting patch serves as a common ground for all PIN diodes, while the control voltage (bias supply) of the individual PIN diodes is applied to the microstrip lines via the separation RF inductors. This is only a schematic drawing, as the exact design of the layout for switching individual PIN diodes is beyond the scope of this paper,

https://doi.org/10.1017/S1759078725000327 Published online by Cambridge University Press

which only aims to present the concept of this star-shaped arrangement of LWA arrays from "Design of a varactor-controlled LWA" section and "Experiment" section, respectively.

The individual LW arrays are fed by DC voltage sources separately as explained above.

Conclusion

The presented 1D LWA array was designed as a reconfigurable array composed of rectangular conducting patches placed on a dielectric substrate (mushroom cells). These patches are intersected by IDCs allowing the connection of varactors that bridge the slits between the patches. This allows the varactors to be powered from a single DC source. The controlled range of maximum radiation angles is 55° as determined by simulations performed by the CST MWS program for a range of varactor capacitances from 0.1 to 1 pF in the frequency band from 8 to 8.2 GHz. This band is the band in which the beam is steered, as described above in Figs. 4 and 9, at 8 GHz, the design frequency. The MA46H120 varactors used are recommended to operate at a DC bias voltage between 0 and 12 V, which corresponds to a capacitance range of 1 to 0.15 pF. This limits the range of measured elevation angles to 40°. The frequency band defined by $S_{11} < -10$ dB is 1.5 GHz and depends in detail on the DC bias voltage defining the capacitances of the varactors. The proposed antenna has a compact size and a simple structure that has been fabricated inexpensively by a printed circuit board procedure. The originality of the presented reconfigurable antenna array lies in its ability to be integrated into complex systems, as has been documented for an electronically steerable full-hemisphere beam antenna.

The presented antenna was assembled in a star configuration. Eight antennas were connected in a star structure with a central feed. The radiation patterns of these individual antennas are switched by PIN diodes to determine the specific azimuthal sector of radiation. The radiation in elevation is controlled by the DC bias of the varactors of the particular antenna array that is switched on at any given time. This reconfigurable antenna therefore represents the original antenna with the direction of the main radiation pattern electronically steerable throughout the hemisphere at a constant frequency.

Acknowledgement. This work was funded by the Czech Science Foundation through the project number GA23-07518S.

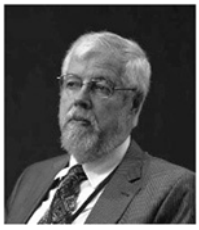
Competing interests. The authors declare none.

References

1. **Lee C-J, Leong KMKH and Itoh T** (2006) Composite right/left-handed transmission line based compact resonant antennas for RF module integration, IEEE. *IEEE Transactions on Antennas and Propagation* **54**(8), 2283–2091.
2. **Lai A, Itoh T and Caloz C** (2004) Composite right/left-handed transmission line metamaterials. *IEEE Microwave Magazine* **5**(3), 34–50.
3. **Beneck RJ, Das A, Mackertich-Sengerdy G, Chaky RJ, Wu Y, Soltani S and Werner DH** (2021) Reconfigurable antennas: A review of recent progress and future prospects for next generation. *Progress In Electromagnetics Research* **171**, 89–121.
4. **Lim S, Caloz C and Itoh T** (2004) Metamaterial-based electronically controlled transmission-line structure as a novel leaky-wave antenna with tunable radiation angle and beamwidth. *IEEE Transactions on Microwave Theory & Techniques* **52**(12), 2678–2690.
5. **Chen K, Zhang YH, He SY, Chen HT and Zhu GQ** (2019) An electronically controlled leaky-wave antenna based on corrugated SIW structure with fixed-frequency beam scanning. *IEEE Antennas and Wireless Propagation Letters* **18**(3), 551–555.
6. **Wang M, Ma HF, Zhang HC, Tang WX, Zhang XR and Cui TJ** (2018) Frequency-fixed beam-scanning leaky-wave antenna using electronically controllable corrugated microstrip line. *IEEE Transactions on Antennas and Propagation* **66**(9), 4449–4457.
7. **Fu JH, Li A, Chen W, Lv B, Wang Z, Li P and Wu Q** (2017) An electrically controlled CRLH-inspired circularly polarized leaky-wave antenna. *IEEE Antennas and Wireless Propagation Letters* **16**, 760–763.
8. **Xu G, Eleftheriades GV and Hum SV** (2022) Wide-angle beam-steering and adaptive impedance matching with reconfigurable nonlocal leaky-wave antenna. *IEEE Open Journal of Antennas and Propagation* **3**, 1141–1153.
9. **Torabi E, Rozhkova A, Chen PY and Erricolo D**, "Compact and reconfigurable leaky wave antenna based on a tunable substrate integrated embedded metasurface," *2020 IEEE Inter. Symp. Antennas Propag. and North American Radio Science Meeting*, 2020.
10. **Martini E, Pavone SC, Albani M, Maci S, Martorelli V, Giodanengo G, Ferraro A, Beccherelli R, Toso G and Vecchi G**, "Reconfigurable antenna based on liquid crystals for continuous beam scanning with a single control," *2019 IEEE Int. Symp. Antennas Propag. and USNC-URSI Radio Science Meeting*, 2019.
11. **Guirado R, Perez-Palomino G, Carrasco E, de la Rosa P and Quintana X** (2024) Electronically reconfigurable reflectarray antenna based on single-layer liquid crystal with independent dual-polarization control. *IEEE Transactions on Antennas and Propagation* **72**(7), 5626–5636.
12. **Zvolensky Z, Chicherin D, Räisänen A, Simovski C, Sterner M, Oberhammer J and Hakojärvi H** (2011) Leaky-wave antenna at 77 GHz. *2011 41st European Microwave Conference* pp. 1039–1042.
13. **Zheng W, Wang J, Zhao H, Li Z, Geng Y, Li Y, Chen M and Zhang Z** (2023) A leaky wave antenna with capability of fixed-frequency beamforming scanning. *IEEE Transactions on Antennas and Propagation* **71**(9), 7585–7590.
14. **Wu C, Ma Y, Venkatesh S, Mehlman Y, Ozatay M, Wagner S, Sturm JC and Verma N** (2024) A monolithically integrable reconfigurable antenna based on large-area electronics. *IEEE Journal of Solid-State Circuits* **59**(5), 1475–1485.
15. **Sabapathy T, Jamlos MF, Ahmad RB, Jusoh M, Jais MI and Kamarudin MR** (2013) Electronically reconfigurable beam steering antenna using embedded RF PIN based parasitic arrays (ERPPA). *Progress In Electromagnetics Research* **140**, 241–261.
16. **You J and Dong Y** (2024) Smart Wi-Fi antenna with reconfigurable omnidirectional and unidirectional patterns. *IEEE Antennas Wireless Propag Lett* **23**(3), 1010–1014.
17. **Nakano H, Abe T and Yamauchi J** (2019) Planar reconfigurable antennas using circularly polarized metalines. *IEEE Antennas and Wireless Propagation Letters* **18**(5), 1006–1010.
18. **Sheel S and Coetzee JC**, "Switchable-feed reconfigurable ultra-wide band planar antenna." *2015 International Symposium on Antennas and Propagation (ISAP)*.
19. **Roychoudhary J, Dutta K, Chatterjee A, Chakrabarti S and Mittra R**, "An edge-tapered antipodal beam switching antenna with 360o azimuthal beam steering," *2024 IEEE International Symposium on Antennas and Propagation*, AP-S/INC-USNC-URSI, 1861–1862, APS 2024.
20. **Rezaee B, Farahani HS and Bösch W**, A novel reconfigurable planar switched-beam filtenna with 360-degree beam scanning, *2024 18th European Conference on Antennas and Propagation (EuCAP)*, 2024.
21. **Sheel S and Coetzee JC**, "Electronically-reconfigurable horizontally polarized wide-band planar antenna," *2015 International Symposium on Antennas and Propagation (ISAP)*.
22. **Zhang Y, Han Z, Tang S, Shen S, Chiu C-Y and Murch R** (2022) A highly pattern-reconfigurable planar antenna with 360o single- and multi-beam steering. *IEEE Transactions on Antennas and Propagation* **70**(8), 6490–6504.

https://doi.org/10.1017/S1759078725000327 Published online by Cambridge University Press

23. **Machac J, Svanda M, and Kabourek V** (2023) A reconfigurable leaky wave antenna. *International Conference Radioelektronika* **2023**(33rd), pp. 1–4
24. **CST Microwave Studio**, [Online]. Available: https://www.3ds.com/products-services/simulia/products/cst-studio-suite,https://www.3ds.com.
25. **Sabah C, Urbani F and Uckun S** (2007) Frequency dependence of bloch impedance in lefthanded transmission line. *The Second Europ.Conf. Antennas Propag*. EuCAP.
26. https://www.macom.com/products/product-detail/MA46H120
27. https://www.rogerscorp.com/advanced-electronics-solutions
28. https://www.nsi-mi.com
29. https://www.rfspin.com/product/drh20e
30. **Machac J, Svanda M, and Kabourek V** (2024) Leaky wave antenna on substrate integrated waveguide with radiation pattern controlled by DC voltage. *International Journal of Microwave and Wireless Technologies* **14**(4), 588–594.



Jan Machac is currently a Professor with the Department of Electromagnetic Field, Faculty of Electrical Engineering, Czech Technical University in Prague, Czech Republic. He is the author or a coauthor of more than 250 publications in scientific journals and scientific international and national conferences. His main scientific interests include planar passive elements and subsystems of microwave technology, planar antennas, and microwave filters, propagation of electromagnetic waves in periodic, and artificial electromagnetic structures, chipless RFID, and power wireless transport.



Milan Svanda received the M.S. and Ph.D. degrees in radioelectronics from Czech Technical University in Prague, in 2007 and 2011, respectively. He currently a Research Scientist with CTU in Prague. He is the author or a co-author of more than 60 articles published in international journals or conference proceedings and co-author of eight patents. His main research activities are focused on antennas operating in close proximity to the human body, low-profile, and wearable RFID and sensor antennas.



Vaclav Kabourek was born in 1985. He received his M.Sc. and Ph. D. degree from the Czech Technical University in Prague in 2010 and 2017. His research interests include antenna design and measurement, RCS measurement. His contemporary research activities are also focused on EMC measurements.

https://doi.org/10.1017/S1759078725000327 Published online by Cambridge University Press